ELSEVIER

Journal of Nuclear Materials 258–263 (1998) 1725–1729

journal of nuclear materials

High-cycle fatigue tests of modified 316 stainless steels under 20 MeV proton irradiation and thermal pulses

H. Mizubayashi [a,*], K. Tateishi [a], H. Tanimoto [a], K. Nakata [b]

[a] *Institute of Materials Science, University of Tsukuba, Tsukuba, Ibaraki 305, Japan*
[b] *Hitachi Research Laboratory, Hitachi Ltd., Hitachi, Ibaraki 317, Japan*

Abstract

In situ radiation damage and thermal pulses considerably modify the high cycle fatigue property of solution treated specimens of the modified 316L stainless steels, where the observed effects show a characteristic relationship with the chemical composition of the specimens. For the specimens which show a low work-hardening exponent, the fatigue life elongates under irradiation. In contrast, the fatigue life of the specimens which show a high work-hardening exponent is shortened under irradiation. A probable dislocation–defect interaction responsible for these effects is discussed.

1. Introduction

The first wall of a fusion reactor is planned to be subjected to thermal stresses and 14 MeV neutron irradiation simultaneously. On the low cycle fatigue property, an effect of in situ radiation damage is negligible because the expected damage rate is too low to modify a violent dynamic defect process under the low cycle fatigue strains or stresses. On the other hand, the high cycle fatigue property is expected to be modified by in situ radiation damage because a dynamic defect process under the high cycle fatigue strains or stresses can be comparable with the damage rate (e.g. [1–8]). Since most of the structural reactor materials are expected to be subjected to the high cycle fatigue strains or stresses during the reactor operation, understanding of the effects of in situ radiation damage and in situ thermal pulse on the high fatigue property is important.

The preliminary high cycle fatigue tests on the Ti-modified AISI 316L stainless steel (316(ST − 1) [4], seen in Table 1 and Fig. 4(a)) indicate that the effect of radiation damage on the fatigue life N_f in the ε_t-controlled tests at 333 K is much larger under irradiation than after irradiation, where ε_t is the total strain amplitude. The further high cycle fatigue tests of various modified-316L stainless steels (316F and 316SI [9–11], seen in Table 1 and Fig. 4(b)) indicate that for the solution treated specimens the chemical composition mainly governs the fatigue hardening process and in situ radiation damage modifies the fatigue hardening process, resulting in the characteristic relationship between the effects of in situ radiation damage on the fatigue life N_f and the chemical composition of the specimens. In the present paper, these results will be reported together with further fatigue tests on 316SI specimens.

2. Experimental

Specimens were cut from the rolled sheets of 316SI with the chemical composition shown in Table 1. The chemical composition of 316(ST−1) reported in Ref. [4] and that of 316F reported in Ref. [9] are also compiled in Table 1, and the present results will be discussed together with the previous results on 316(ST − 1) and 316F specimens. As will be shown in Fig. 4(a) and (b), the work hardening exponent n [12] is the highest in 316SI, the lowest in 316(ST − 1) and intermediate in 316F. After mechanical polishing, 316SI specimens were annealed at 1370 K for 3.6 ks in a vacuum of 2×10^{-4} Pa and then quenched into water. As quenched specimens were electrolytically polished in order to remove

* Corresponding author. Tel.: +81 298 53 5063; fax: +81 298 55 7440; e-mail: mizuh@mat.ims.tsukuba.ac.jp.

0022-3115/98/$19.00
PII: S0022-3115(98)00295-5

Table 1
Chemical composition of the material used (mass%)

Material	C	Si	Mn	P	S	Cr	Ni	Mo	N	Ti
316SI [a]	0.005	1.38	1.35	0.014	0.009	17.32	13.59	2.34	0.001	–
316F [a]	0.038	0.04	0.23	0.003	0.002	16.77	13.95	2.32	0.011	–
316(ST-1) [a]	0.077	1.00	1.81	0.029	< 0.003	16.20	13.60	2.46	–	0.089

[a] Modified AISI 316L stainless steels, where the codes indicated are used only to refer to the specimens with the given chemical composition.

the surface layer of about 0.05 mm and to smooth out the surfaces, and then annealed again at 573 K for 36 ks in a vacuum of 2×10^{-4} Pa to degas hydrogen picked up during the electrolytical polishing. The grain size was typically 0.05 mm.

The fatigue tests were carried out using the flexural vibrations of a U-shaped reed specimen, where the middle of the U-shape forms a composite reed with thickness of 0.12 mm and a gage length of 16 mm and two open ends of the U-shape are thick for clamping. Excitation of the flexural vibrations was made electromagnetically and the fatigue tests were conducted in the atmosphere of 10^2 Pa He to suppress a heat-up of a specimen (see Refs. [4,10] for details). Period P of the resonant flexural vibrations of a specimen in the elastic range will be referred to as P_0 below, where $1/P_0$ is about 200 Hz. The fatigue tests were started by an increase in the total strain amplitude ε_t beyond microyielding. For the ε_t-controlled tests (see Ref. [4] and Fig. 4(a) for 316(ST − 1)), P shows a strong increase during several thousands cycles after the increase in ε_t, and then starts to decrease due to the fatigue hardening, where the plastic strain amplitude ε_p is proportional to $(P - P_0)/P_0$. With increasing fatigue cycles, the fatigue hardening tends towards saturation and at the fatigue cycles of about $0.9N_f$, P starts to increase reflecting a decrease in the cross-sectional area of the specimen due to the start of crack propagation. That is, for smooth specimens, most of N_f is governed by the dislocation behavior. In the present plastic strain amplitude, ε_p, controlled tests, P was held at a given value P_h by adjusting the total strain amplitude, ε_t, during the fatigue hardening and then, after the saturation of the fatigue hardening, ε_t was kept at an attained ε_t. The fatigue tests without proton irradiation or thermal pulses will be referred to as the no-load tests (the NL-tests), hereafter. For the thermal pulse tests (the TP-tests), a thermal pulse ΔT of 10 s was given every 30 s using a halogen lamp light, where the specimen temperature rises to 90% of the ultimate ΔT in a few seconds. For the proton irradiation tests (the PI-tests) or the pulse-PI-tests, irradiation was made using 20 MeV protons of 0.02–0.03 A/m^2 from the tandem accelerator at the University of Tsukuba, where the radiation damage rate estimated is about 1×10^{-7} dpa/s for 0.025 A/m^2. The present fatigue tests were conducted at 300 and 403 K.

3. Results

Fig. 1 shows the $(P_h - P_0)/P_0$ vs. N_f data observed for 316SI specimens; the NL-tests at 300 K [11] and 333 K [10], the TP-tests at 333 K with ΔT below 10 K [10] and the TP-tests at 300 K with $\Delta T = 70$–130 K [11]. The low cycle NL-tests on 316L stainless steel reported in Ref. [13] indicate that the dependence of N_f on ε_p is insensitive to the testing temperatures. In the present high cycle NL-tests on 316SI specimens, as will be shown in Fig. 3, the dependence of N_f on $(P_h - P_0)/P_0$ is insensitive to the testing temperatures. Therefore, the $(P_h - P_0)/P_0$ vs. N_f data for the NL-tests at 300 K and those at 333 K will be put into one group as the NL-tests at 300–333 K, hereafter. As seen in Fig. 1, the TP-tests with ΔT below 10 K brings about elongation of N_f but the TP-tests with increased ΔT of 70–130K gives rise to shortening of N_f. The SEM observation of the specimen surfaces (not shown here) indicates that the areal density of slip bands observed after the TP-tests with ΔT below 10 K is higher than, and that after the TP-tests with ΔT of 70–130 K is lower than after the NL-tests, respectively.

Fig. 2 shows the $(P_h - P_0)/P_0$ vs. N_f data observed for the pulse-PI-tests at 333 K on 316SI specimens [10], which are compared with the $(P_h - P_0)/P_0$ vs. N_f data for the TP-tests with ΔT below 10 K shown in Fig. 1 because the present pulse proton irradiation was accompanied by a thermal pulse with ΔT below 10 K. It is seen in Fig. 2 that for 316SI specimens the in situ radiation damage at 333 K causes shortening of N_f, especially in the low $(P_h - P_0)/P_0$ range around $(P_h - P_0)/P_0 = 0.12$. The SEM observation of the specimen surfaces (not shown here) indicates that the areal density of slip bands observed after the pulse-PI-tests is lesser than after the TP-tests with ΔT below 10 K, especially for the low $(P_h - P_0)/P_0$ range around $(P_h - P_0)/P_0 = 0.12$.

Fig. 3 shows the $(P_h - P_0)/P_0$ vs. N_f data observed for the NL-tests at 403 K and the PI-tests at 403 K on 316SI specimens, where a redrawing of the $(P_h - P_0)/P_0$ vs. N_f data for the NL-tests at 300–333 K are also given. Although the areal density of slip bands observed after the NL-tests at 403 K was much higher than after the NL-tests at 300–333 K (not shown here), the dependence of N_f on $(P_h - P_0)/P_0$ found for the NL-tests at 403 K was very similar to that for the NL-test at 300–333 K.

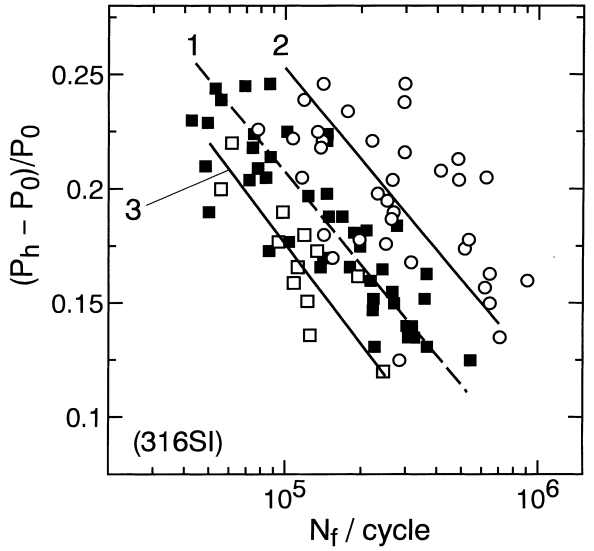

Fig. 1. $(P_h - P_0)/P_0$ vs. N_f observed for the high-cycle fatigue tests at 300–333 K for 316SI specimens (see text): ■,1 = NL-tests; ○,2 = TP-tests with ΔT below 10 K; □,3 = TP-tests with ΔT = 70–130 K. The lines 1–3 are tentatively fitted to the data.

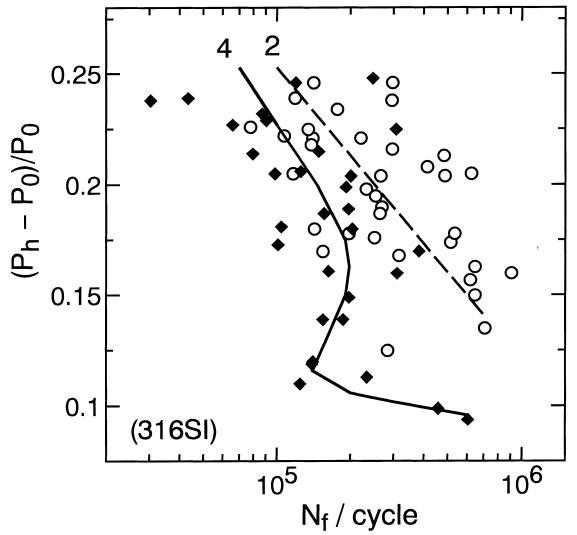

Fig. 2. $(P_h - P_0)/P_0$ vs. N_f for the pulse-PI-tests at 333 K of 316SI specimens (♦,4) is compared with that for the TP-tests with ΔT below 10 K shown in Fig. 1 (○,2). The lines 2 and 4 are tentatively fitted to the data, see [10].

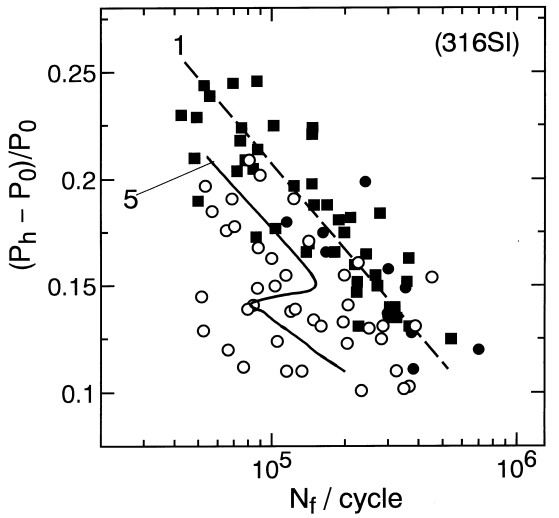

Fig. 3. $(P_h - P_0)/P_0$ vs. N_f for the PI-tests at 403 K of 316SI specimens (○,5) is compared with that for the NL-tests at 403 K of 316SI specimens (●,1), where $(P_h - P_0)/P_0$ vs. N_f for the NL-tests at 300–333 K (■,1) is also plotted. The lines 1 and 5 are tentatively fitted to the data.

The effect of the in situ radiation damage on the dependence of N_f on $(P_h - P_0)/P_0$ at 403 K is very similar to that found at 333 K, i.e. the in situ radiation damage causes shortening of N_f, especially in the low $(P_h - P_0)/P_0$ range around $(P_h - P_0)/P_0 = 0.14$. The results for the SEM observation of the specimen surfaces after the PI-tests at 403 K (not shown here) are also very similar to those mentioned for the pulse-PI tests, i.e. the areal density of slip bands observed after the PI-tests is lower than after the NL-tests, especially for the low $(P_h - P_0)/P_0$ range around $(P_h - P_0)/P_0 = 0.14$.

4. Discussion

Fig. 4(a) shows the ε_t vs. N_f data for the NL-tests and the PI-tests at 333 K on 316(ST − 1) specimens reported in Ref. [4]. Fig. 4(b) shows the $(P_h - P_0)/P_0$ vs. N_f data

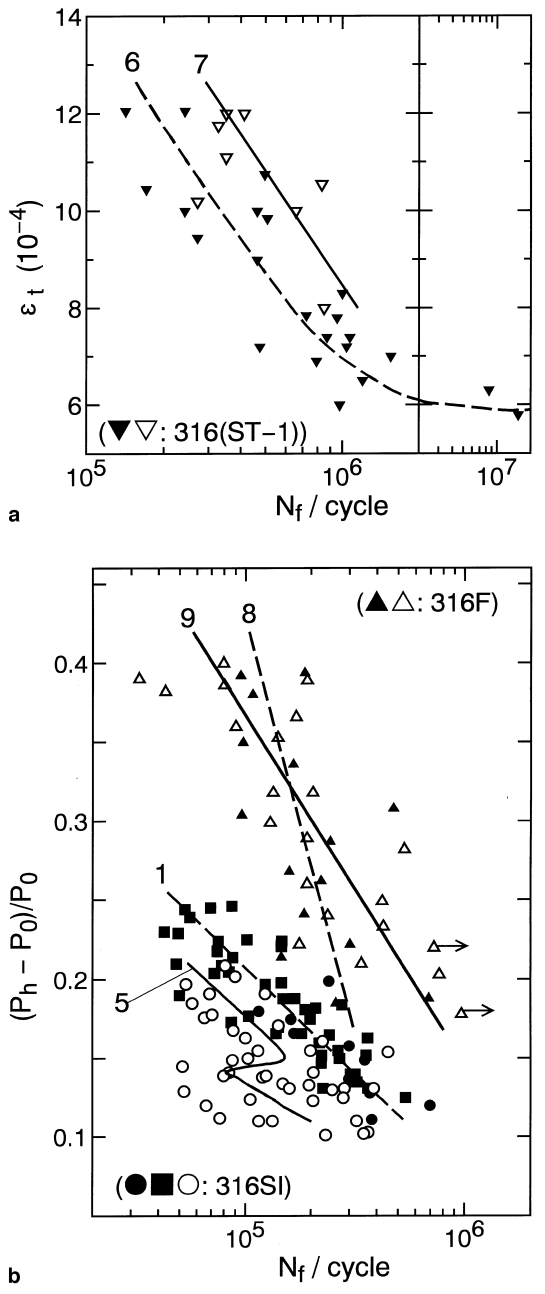

Fig. 4. (a) For 316(ST-1) specimens, ϵ_t vs. N_f for the PI-tests at 333 K of (▽,7) is compared with that for the NL-tests (▼,6), The lines 6 and 7 are tentatively fitted to the data, see [4]. (b) $(P_h - P_0)/P_0$ vs. N_f for the PI-tests (△,9) and that for the NL-tests (▲,8) at 333 K of 316F specimens [9] are compared with $(P_h - P_0)/P_0$ vs. N_f for the PI-tests and the NL-tests at 403 K of 316SI specimens shown in Fig. 3.

for the NL-tests and the PI-tests at 333 K on 316F specimens reported in Ref. [9], where a redrawing of the $(P_h - P_0)/P_0$ vs. N_f data for 316SI specimens shown in Fig. 3 is also given. The work hardening exponent n [12] estimated from the N_f data for the NL-tests is about 1 for 316SI, about 0.3 for 316F and about 0.2 for 316(ST − 1), respectively. In 316(ST − 1) specimens, the fatigue hardening observed in the high cycle fatigue tests is mainly governed by the fatigue enhanced precipitation [9], resulting in a low value of the work hardening exponent. Further the precipitates are too large to be dispersed by 20 MeV proton irradiation [9], suggesting that the elongation of N_f in the ε_t-controlled PI-tests observed in 316(ST − 1) specimens reflects enhancement of the fatigue hardening under proton irradiation which causes a decrease in the constituent plastic strain amplitude in the ε_t-controlled tests.

In contrast, for 316SI specimens, the work hardening exponent is as high as 1 and on the specimen surface after the fatigue tests well-developed slip bands are observed with a high areal density. The morphology of slip bands in 316SI is similar to that of persistent slip bands (PSBs) in annealed copper specimens after the NL-tests, except that the width and height of a slip band in 316SI specimens are considerably less than those of a PSB in copper specimens. It is known that for the ε_p-controlled tests, an increase (a decrease) in the areal density of PSBs brings about a decrease (an increase) in the local-ε_p in PSBs, resulting in elongation (shortening) of the fatigue life. The close relationship between the surface morphology and the $(P_h - P_0)/P_0$ vs. N_f data observed in 316SI specimens suggests that an effect of proton irradiation or thermal-pulses on PSBs governs their effects on the fatigue life. For the elongation of N_f in the TP-tests with ΔT of 10 K, we suppose that the local-ε_p in PSBs was not equal among PSBs and the PSBs with a lower local-ε_p could preferentially be activated under thermal pulses with ΔT of 10 K through dislocation rearrangements. It is noted that the heart of the TP-tests is an abrupt change in specimen temperatures, i.e. gradual changes in the specimen temperatures hardly modify N_f. In contrast, for the TP-tests at 300 K with $\Delta T = 70$–130 K, one can expect both dislocation rearrangements and an introduction of the fatigue induced precipitates (see Fig. 6 in Ref. [10]) during thermal pulses. The decrease in N_f for the TP-tests with $\Delta T = 70$–130 K shown in Fig. 1 suggests that the effect of the fatigue induced precipitation is predominant for the TP-tests. Both the shortening of N_f in 316SI specimens due to in situ radiation damage at 333 K shown in Fig. 2 and that at 403 K shown in Fig. 3 are surmised to be related to irradiation induced hardening. The strong shortening of N_f due to in situ radiation damage around $(P_h - P_0)/P_0 = 0.12$ at 333 K shown in Fig. 2 and that around $(P_h - P_0)/P_0 = 0.14$ at 403 K shown in Fig. 3 possibly indicate that the irradiation induced precipitation takes place in 316SI, where the precipitates can be dispersed by dislocation motions when the plastic strain amplitude during the fatigue tests is increased.

The work hardening exponent and the effect of in situ radiation damage on N_f in 316F shown in Fig. 4(b) are intermediate between those in 316SI and in 316(ST − 1). These results indicate the close relationship between the effect of in situ radiation damage on the fatigue life and the chemical composition. To clarify this issue, further work is now in progress.

5. Conclusion

From the high cycle fatigue tests on solution treated smooth specimens of modified 316L stainless steels, the close relationship between the effect of in situ radiation damage on the fatigue life and the chemical composition of the specimens is found. The present work demonstrates that understanding of the effect of in situ radiation damage on the fatigue property is important for the first wall materials.

Acknowledgements

The authors are grateful to the staff of the Tandem Accelerator Center of the University of Tsukuba for their invaluable help during the course of irradiation experiments. This work is partly supported by a Grant in Aid for Scientific Research from the Ministry of Education, Science and Culture of Japan.

References

[1] K. Sonnenberg, H. Ullmaier, J. Nucl. Mater. 102 (1981) 333.
[2] A.M. Ermi, B.A. Chin, J. Nucl. Mater. 103–104 (1981) 1505.
[3] J. Weerman, W.V. Green, J. Nucl. Mater. 97 (1981) 254.
[4] H. Mizubayashi, S. Okuda, K. Nakagome, H. Shibuki, S. Seki, Mater. Trans. Jpn. Inst. Metals 25 (1984) 257.
[5] K. Ehrich, J. Nucl. Mater. 133/134 (1985) 119.
[6] P. Jung, H. Ullmaier, J. Nucl. Mater. 174 (1990) 253.
[7] M.L. Grossbeck, K. Ehrich, C. Wassilew, J. Nucl. Mater. 174 (1990) 264.
[8] R. Lindau, A. Moeslang, J. Nucl. Mater. 179–181 (1991) 753.
[9] H. Mizubayashi, T. Fujita, S.-C. Yan, S. Okuda, Mater. Trans. Jpn. Inst. Metals 32 (1991) 539.
[10] H. Mizubayashi, K. Ikemi, H. Tanimoto, S. Okuda, Mater. Trans. Jpn. Inst. Metals 33 (1992) 816.
[11] H. Mizubayashi, K. Tateishi, H. Tanimoto, K. Nakata, J. Phys. (Paris) IV 6 (1996) C8–853.
[12] P. Marshall, Austenitic Stainless Steels; Microstructure and Mechanical Properties, Elsevier, London, 1984, p. 175.
[13] K. Furuya, N. Nagata, R. Watanabe, J. Nucl. Mater. 89 (1980) 372.